2011 31st International Conference on Distributed Computing Systems

# SID: Ship Intrusion Detection with Wireless Sensor Networks

Hanjiang Luo*‡, Kaishun Wu†§, Zhongwen Guo*, Lin Gu†, Zhong Yang‡ and Lionel M. Ni†ι
*Department of Computer Science, Ocean University of China
†Department of Computer Science & Engineering, Hong Kong University of Science and Technology
‡Department of Information Engineering, Zibo Vocational Institute, Zibo, China
§School of Physics and Engineering, Sun Yat-sen University, Guangzhou, China
ιShanghai Key Lab of Scalable Computing and Systems, Shanghai Jiao Tong University, Shanghai, China
Email: {luo.wireless}@gmail.com, {guozhw, luohj}@ouc.edu.cn, {kwinson, lingu, ni}@cse.ust.hk

***Abstract*—Surveillance is a vital problem for harbor protection, border control or the security of other commercial facilities. It is particularly challenging to protect the vast near-coast sea surface and busy harbor areas from intrusions of unauthorized marine vessels, such as trespassing boats and ships. In this paper, we present an innovative solution for ship intrusion detection. Equipped with three-axis accelerometer sensors, we deploy an experimental wireless sensor network on the sea surface to detect ships. Using signal processing techniques and cooperative signal processing, we can detect the passing ships by distinguishing the ship-generated waves and the ocean waves. We design an intrusion detection system in which we propose to exploit spatial and temporal correlations of the intrusion to increase detection reliability. We conduct evaluations with real data collected by our initial experiments, and provide quantitative analysis on the detection system, such as the successful detection ratio and the estimation of the intruding ship velocity.**

***Keywords*-Ship detection; wireless sensor networks; harbor protection;**

## I. Introduction

Intrusion detection on the sea is a critical surveillance problem for harbor protection, border security, and commercial facilities protection, such as oil platforms and fisheries facilities. Though there are intrusion objects underwater (e.g., scuba divers), surface threats such as boats or ships are more common.

The traditional methods of detecting ships are with radars or satellites which are very expensive. Except the high cost, the satellite image is easily affected by the cloud. And it is difficult to detect small boats or ships on the sea with marine radar due to the noise or clutters generated by the uneven sea surface.

Wireless sensor networks (WSNs) are developed for terrestrial intrusion detection recently [1]–[3]. These networks deploy sensors, such as magnetometers, thermal sensors, and acoustic sensors, in the monitored area to detect intruders [1], [4]. Though such networks may work well on the land, it is challenging to deploy these sensors on the sea surface for ship detection.

The main challenge is that when sensors are deployed on the sea surface, they are not static and tossed by ocean waves which make the sensors move around randomly [5]. These movements make most sensors, (e.g., magnetometers and thermal sensors), difficult to detect the intrusion. Due to the high cost and stability requirement, using the camera sensors is not a general solution in such scenarios [6]. For the same reason mentioned earlier, the detection results can also be easily affected by the random movement of the cameras.

Figure 1: Experimental sensor network deployment

When a ship moves through the water, it generates V-shaped waves [7]. Though the studying of the ship-generated waves has been an old research topic which mainly focused on the harm of these waves, such as reducing wave resistance for ship hull design, or preventing damage of coastal or marine floating structures [8], the investigation of the characteristics of ship waves propagated to large distances from a ship has not been the focus area in most of the research projects.

In this paper, we leverage the characteristics of ship-generated waves for ship detection. We have conducted experiments to detect ship-generated waves. To the best of our knowledge, this is the first detailed, systematic experimental study of ship intrusion detection with WSNs. We summarize the main contributions of this paper as follows:

1. We have proposed a novel approach for ship detection by taking advantage of the characteristics of ship-generated waves with WSNs.

2. We have deployed an experimental WSNs to detect

1063-6927/11 $26.00 © 2011 IEEE
DOI 10.1109/ICDCS.2011.21

Figure 2: Wave generated by a passing boat

ships by using three-axis accelerometer sensors with iMote2 on buoys on the sea surface as shown in Fig. 1. Using signal processing, we observe that the ocean waves and ship-generated waves have different energy spectrum.

3. We have designed an intrusion detection system to detect ships with intrusion characteristics. In the system, we propose to exploit spatial and temporal correlations of the intrusion to increase detection reliability.

4. We have conducted evaluations with real data collected by our initial experiments, and provide quantitative analysis of the detection system, such as the successful detection ratio and the estimation of the speed of the intruding ships.

The paper is organized as follows. In Section II, we introduce the characteristics of ship-generated waves. Distinguishing between ship-generated waves and ocean waves is described in Section III. The design of the detection system is presented in Section IV. In Section V, we provide the performance evaluation. We survey the related work in Section VI. Finally, conclusions are presented and suggestions are made for future research in Section VII.

## II. Preliminaries: the ship-generated waves

The research on ship waves generated by the forward motion of marine vessels, as shown in Fig. 2, is of great interest over the past few decades to vessel designers and environmentalists. The traditional research mainly focused on reducing wave resistance or preventing damage of coastal structures [8].

In this section, we describe both the ship wave patterns and the decay of the ship waves.

### A. The ship wave patterns

When a ship moves across the surface of water, it generates waves which consist of divergent and transverse waves as shown in Fig. 3. The wake pattern was first presented mathematically by Lord Kelvin [7], and he found that the V-shaped pattern was formed by two locus of cusps whose angle with the sailing line is $19°28'$ in deep water. According to his theory, the angle between the sailing line and the diverging wave crest lines at the cusp locus line should be $54°44'$. Note that this pattern is independent of the size and velocity of the ship.

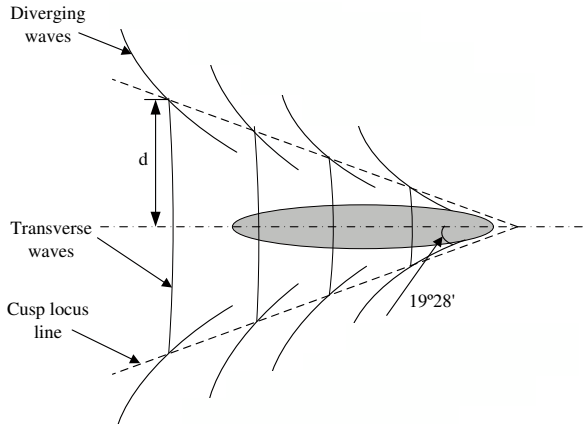


Figure 3: Ship-generated wave model

### B. The decay of ship waves

When the ship waves spread out sideways and propagate from the sailing line, both the height and energy of the waves decrease. Some studies show that the waves height at the cusp points decreases inversely proportional to the cube root of the distance from the vessel [9], [10]. The research in [9] pointed out that the transverse waves decrease inversely proportional to the square root of the distance from the vessel, which means that transverse waves decay much faster than divergent waves. Only divergent waves can be observed far from the vessel. In addition, when we observe the ship-generated waves at a fixed spatial point, the ship-generated wave train has a limited duration [11].

The maximum wave height $H_m$ at distance $d$ from the sailing line can be expressed as the following equation:

$$H_m = cd^{-\frac{1}{3}}. \tag{1}$$

where $c$ is a parameter related to the speed of the passing ship. The ship waves attenuate to background wave level as the waves travel away from the sailing path, and the speed of the ship-wave $W_v$ can be predicted by the following equation:

$$W_v = V \times cos\Theta \tag{2}$$

where $V$ is the speed of ship, and $\Theta = 35.27(1-e^{12(F_d-1)})$ ($F_d$ is the Froude number related to the traveling ship).

In next section, we use accelerometer to measure ship waves.

## III. Distinguish between ship-generated waves and ocean waves

As mentioned in Section I, the movement of sensors on the sea surface makes them difficult to detect the intrusion target. Observing the ship-generated waves when a ship is traveling on the water, we intend to detect ships by detecting these waves generated by the traveling ship. However, in

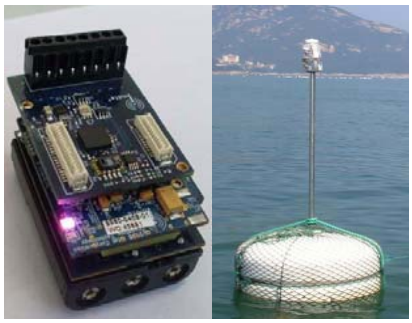

Figure 4: IMote2 sensor and a deployed sensor buoy

order to detect ships via their generated waves, we have to distinguish the ship-generated waves from the ocean waves.

In this section, we first discuss how to measure the ship-generated waves with accelerometer sensors, and then use signal processing techniques to distinguish between ship-generated waves and ocean waves.

### A. Experiment deployment

The experiment hardware used to detect ship waves is from Crossbow, which composed of IMote2 Processor Radio Board (IPR2400) and Basic Sensor Board (ITS400), as shown in Fig. 4. The Basic Sensor Board contains a three-axis ST Micro LIS3L02DQ accelerometer, an advanced temperature/ humidity sensor, a light sensor and a 4 channel A/D converter. The accelerometer has a range of +/-2g with 12 bit resolution [12]. We mount the sensor node into a bottle, and fix the bottle on a buoy. A deployed sensor buoy is shown in Fig. 4.

To deploy a surveillance wireless sensor networks, the sensor nodes are either deployed randomly or manually over a given monitored field. In our deployment, we choose to deploy sensor nodes manually in grid fashion as shown in Fig. 9. The nodes are time-synchronized before deployment, and the locations of the nodes are assigned at the time when they are deployed. The accelerometer on the buoy measures three-axis acceleration of the buoy once the buoy is deployed on the sea surface. Testing runs were performed by driving a fishing boat with different speeds across the testing field. The sample rate of the accelerometer is 50Hz.

### B. Measure waves with accelerometers

The most commonly used method of measuring ship-generated waves is to measure the pressure fluctuations at some elevation points in the water column, then transform the pressure into wave height [11]. However, this method needs expensive devices. In addition, it is difficult to deploy the devices underwater.

In this paper, we use accelerometers to measure the actual surface movement of ship waves. The accelerometer generates output signals whose amplitudes are related to the acceleration applied to it. When the accelerometer is used

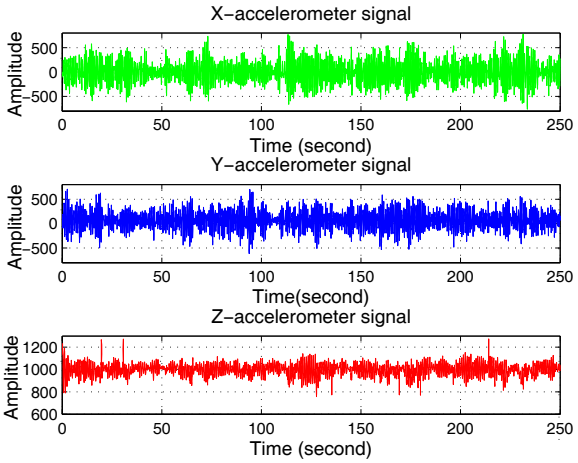


Figure 5: Ocean waves measured by three-axis accelerometer

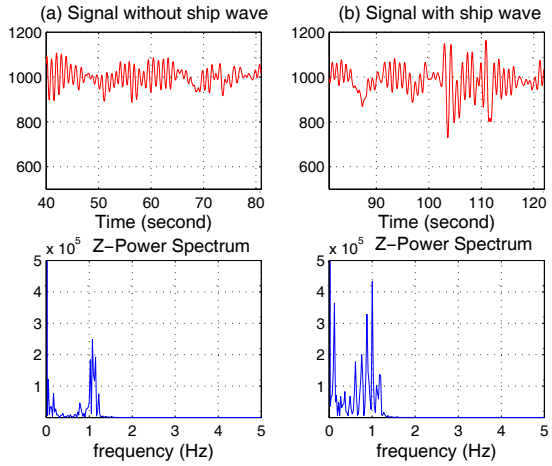


Figure 6: Short-time Fourier transform: (a) Signal without ships and its spectrum. (b) Signal with ships and its spectrum.

in the ocean environment, the buoy and the accelerometer undergo a generally oscillatory, sinusoidal-like vertical acceleration due to wave action. Fig. 5 shows the three-axis ocean wave measurements collected by our experiment sensor networks, which last for a period of 250 seconds. As shown in Fig. 5, the ocean waves change with time. If we use the accelerometer to measure ship-waves, we must distinguish between the ship waves and ocean waves.

Because the sensor changes direction randomly in the ocean, we only consider the z-accelerometer readings in this paper.

### C. The spectrum of the ship waves

In order to distinguish between ship-generated waves and ocean waves, we use Short Time Fourier Transform (STFT)

and wavelet transform to process the measured signals.

*1) Short-time Fourier transform:* Fourier transform is a popular transform method for wave signal analysis. It gives us the full information of spectrum energy of different frequency existed in the entire signal waveform. However, the Fourier transform conceals the frequencies at a particular time. It can not tell when some new frequency signals appear. In other words, we have no time information in the transform. Thus, the Fourier transform is poorly suited to very brief signals, or signals that change suddenly and unpredictably [13].

To solve this problem, we may divide the signals into segments, and for each segment, the Fourier transform can be applied. This approach is called Windowed Fourier Transform or STFT.

With 2048 point sample STFT (40.96s), we observe that ship waves and ocean waves have a different energy spectrum as shown in Fig. 6. Fig. 6(a) shows ocean waves without ship waves. Its spectrum has a high, single peak concentration. On the contrary, the spectrum of the ocean waves combining with the ship waves, as shown in Fig. 6(b), has multiple peaks and wide crests without distinct peaks.

*2) Wavelet analysis:* A problem related to STFT is the finite length of the window. In order to obtain a perfect frequency resolution, the window should be long enough [14]. To achieve a better time resolution, the window should be narrow which makes the frequency resolution less precise. To solve this dilemma, the wavelet transform was proposed [15]. Similar to Fourier analysis as it breaks signal into a series of sine waves of different frequencies, the wavelet transform breaks the signal into mother wavelet which can be scaled and shifted.

We choose a most extensively used mother wavelet which called Morlet wavelet in the wave analysis application. The mother wavelet is expressed as

$$\Psi(t) = exp[-\frac{1}{2}(\frac{t-\tau}{b})^2]exp[ic\frac{b}{t-\tau}] \qquad (3)$$

where $c$ is the frequency of mother wavelet.

The wavelet transform results are presented in Fig. 7. The figure shows that the ship waves mainly focus on the low frequency spectrum. In the next section, we use the characteristic of the ship wave applied to ship intrusion detection system design.

## IV. Ship intrusion detection system design

To design a reliable ship intrusion detection system, we present the architecture of the networks and collaborative signal processing (CSP) in this section. We first present the characteristics of the distributed intrusion detection system, then discuss the system in detail.

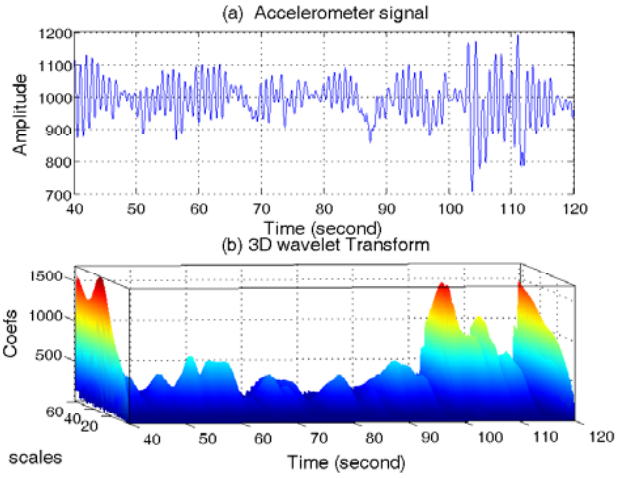


Figure 7: Wavelet transform with 3D plotting: (a) Accelerometer signal. (b) 3D wavelet Transform.

### A. The architecture of the intrusion detection system

A reliable intrusion detection system may involve node-level detection, cluster-level classification, and sink-level classification.

The node-level detection involves sampling the event and processing the sampled data to extract features for the detection. Upon the node detecting the presence of a target in the vicinity of the sensor, it may ideally want to transmit the sampled data to a local head node or a sink for further signal processing and classification. However, due to the energy constraints of the sensor node and the limitation of communication bandwidth, it is better that only the extracted features are transmitted to the local head node.

The cluster-level classification deals with more complicated tasks, such as CSP or regional data fusion. The clusters are formed according to the geographical locations of nodes or the migration of the external "event" after the network deployment [3], [6]. In each cluster, there is a local head node, which is either a normal node or a high energy node, and the head node takes charge of the data fusion or other coordination tasks within the cluster. Some nodes in a group may keep active to perform a coarse detection while other nodes sleep if the networks are densely deployed. Upon a positive detection is made, sleeping nodes should be activated and increase the sampling rate to perform a more accurate detection.

The sink-level detection involves processing the data sent from local head nodes, and the final decision will be reported to the external user via satellite or other means.

To achieve long-term surveillance, some power managements should be used. Meanwhile some middleware services should be considered, such as the location of nodes, time synchronization, and routing infrastructure, etc. [1], [16]–[18].

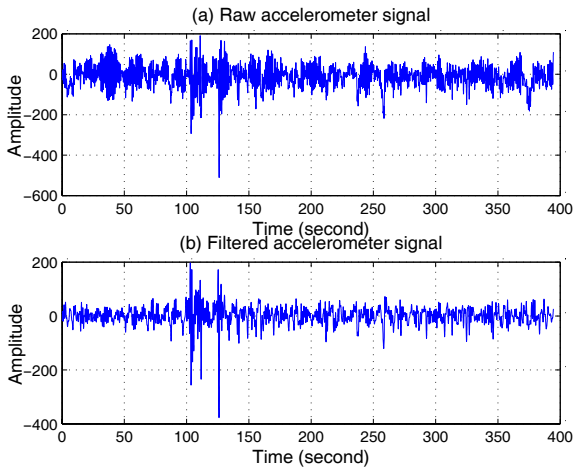


Figure 8: (a) Raw accelerometer signal. (b) Filted accelerometer signal.

For simplicity, we present node-level detection and cluster-level detection in detail here.

### B. Node-level detection

At node-level detection, the task for a single node is to detect ship waves generated by a passing ship nearby. In order to do that, the individual node periodically samples the event and processes the sampled data to extract features for node-level detection. In our scheme, after deployment of the node, the node first samples for a period of time, then filters out the frequency above 1Hz, the results are shown in Fig. 8.

Because the z-accelerometer signal fluctuates around $1g$, we minus this value and let the signal fluctuates around zero. Before computing the average and standard deviation, we have the absolute value of those signal below zero. The reason is that, when the ship waves disturb the buoy, all fluctuations either above $1g$ or below $1g$ contain the disturbance information.

We assume the sample signal value at time $t$ is $a_i$, the total number of sampling point in time period $T$ is $u$. The average sample value of this period $T$ and the standard deviation can be computed as fellows:

$$\begin{cases} m_{\Delta t} = \frac{1}{u}\sum_{i=1}^{u} a_i \\ d_{\Delta t} = \sqrt{\frac{1}{u}\sum_{i=1}^{u}(a_i - m_{\Delta t})^2} \end{cases} \tag{4}$$

Because ocean waves change with wind and time, the threshold should reflect that changing. Thus we design an environment adaptive threshold by moving the average value and the standard deviation with time. The moving average and standard deviation is defined as follows:

$$\begin{cases} m_T^{'} = \beta_1 \times m_T + m_{\Delta t} \times (1-\beta_1) \\ d_T^{'} = \beta_2 \times d_T + d_{\Delta t} \times (1-\beta_2) \end{cases} \tag{5}$$

where $m_{\Delta t}$ and $d_{\Delta t}$ are the historical average and the standard deviation, $\beta_1$ and $\beta_2$ are parameters which are empirically determined to 0.99 here.

We define $D_i$ for each sampled signal $a_i$ as follows:

$$D_i = |a_i - d_T^{'}| \tag{6}$$

The threshold is defined as $D_{max} = Mm_T^{'}$, where $M$=1,2,3. If $D_i > D_{max}$, we consider that the threshold has been crossed.

Because the ship waves actually are train of waves, the disturbance to the sensor should last for a short period of time. In other words, the crossing of the threshold occurs several times within a short period of time $\Delta t$. So, we define anomaly frequency $a_f$ as follows:

$$a_f = \frac{NA_{\Delta t}}{N_{\Delta t}} \tag{7}$$

where $NA_{\Delta t}$ is the number of the crossing occurred during that period of time $\Delta t$, $N_{\Delta t}$ is the total number of samples within time period $\Delta t$.

The average energy of crossing within the period of time $\Delta t$ can be computed as fellows:

$$E_{\Delta t} = \frac{1}{NA_{\Delta t}} \sum_{\Delta t} D_i \quad (D_i > D_{max}) \tag{8}$$

The node reports the detection to a local head node for further signal processing if $a_f$ passes a pre-defined threshold, and it reports $E_{\Delta}$ and the onset time when the signal first exceeds the threshold.

In the next section, we discuss the cluster-level classification.

### C. Cluster-level detection

Though a passing ship can be detected by individual node, many factors affect the detection results in a real-world deployment of an ocean-based surveillance system. For example, wind may affect the sensors and cause a flurry of false positives by directly moving sensors and making "environmental noise". Animal such as birds or fish may also disrupt the sensor readings.

In addition to these noises, other reasons may have an impact on the reliability of the detection system. Some nodes with hardware errors may not detect the ship when it passing. Even with perfect detection, its positive report may not be transmitted back timely due to wireless communication errors [20] and possible network congestions [19].

To improve the detection performance and decrease the false positive rate, it is useful that multiple nodes cooperatively detect the ship. Next, we first present in-network data processing with spatial and temporal correlations between nodes. Then, we estimate the speed of the passing ship with several nodes' cooperatively collected data.

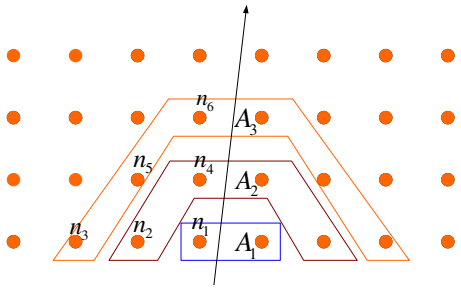


Figure 9: Spatial and temporal correlation

*1) Spatial and temporal correlations:* When a ship travels through the deployed area of the wireless sensor networks, it will disturb a successive of small areas continually. Because of the characteristics of the ship waves as described in section II, these areas have spatial and temporal correlations. By exploiting these spatial and temporal correlations in cluster-level detection, we can improve the reliability of the detection system.

As shown in Fig. 9, when a ship travels through the sensor networks, the waves generated by the passing ship disturb the sensor area $A_1, A_2, A_3$ in a sequential manner.

After the deployment of WSNs, it should run time synchronization and localization algorithms, so nodes know their position and have synchronized time within the network. However, it is not too costly to run synch and localization to reach certain precision required by our application.

In order to monitor the whole deployed area, the network should be partitioned into "cells" by forming static clusters. In this paper, we propose combining temporary clusters with these static clusters. The static clusters are formed according to the geographical location of nodes after the networks' deployment. Meanwhile, we also set up temporary clusters on demand when a node has a positive alarm. Because the node position is fixed, they know their neighbors' position. When a node finds ship intrusion, it initiates the temporary cluster, informs its neighbor nodes within $N$ hops and becomes the temporary cluster head automatically. If the nodes within the cluster also find the intrusion, they report the findings to its temporary cluster head. If the cluster head has not received any reporting within a certain period of time, it will cancel the temporary cluster because its positive finding may be a false alarm. However, if it receives enough positive reporting timely, it will process the received data using the spatial and temporal correlations of ship waves. For example, as shown in Fig. 9, we assume that node $n1$ first detects the ship and initiates a temporary cluster in which it is the cluster head. Within a certain period of time, it receives enough positive reports from its neighbors. Then it can use these reports to find out whether they have spatial and temporal correlations.

The ship will disturb nodes in several rows or columns just as Fig. 9 shows. Because the nodes nearest to the ship's travel line get stronger signal strength than other nodes in each row, all the disturbed nodes can be separated into two sides. For simplicity, we only consider one side of the nodes below.

In each row, we assume that the total number of active nodes ( the node which has positive reports) is $n$. We define $C_{rt(i)}$ as the time correlations in row $i$. Because the cluster head knows the positions of each node, we arrange all reports according to their position and reporting time. For example, in row $i$, if and only if node $a's$ position is closer to the ship travel line and the reporting time is early than node $b's$, we order them. If the number of ordered reports is $N$, $C_{rt(i)}$ is computed as follows:

$$C_{rt(i)} = \frac{N}{n} \tag{9}$$

where $C_{rt(i)} = 1$ if there is only one report in one row.

The group's time correlations $C_{Nt}$ defines as follows:

$$C_{Nt} = \prod C_{rt(i)} \tag{10}$$

where $C_{rt(i)}$ is the time correlations in each row.

$C_{re(i)}$ describes the energy correlations of reports in each row. Because the ship waves attenuate with distance between the ship travel line and the sensor, the nodes closer to the travel line have higher ship-wave energy. This will lead to different average energy $E_{\Delta t}$. We order all reports according to their positions and average energy. For example, in row $i$, if and only if node $a's$ position is closer to the ship travel line than node $b$, and $E_{\Delta t}(a) > E_{\Delta t}(b)$ , we order them. If the number of sorted reports is $N$, $C_{re(i)}$ is defined as follows:

$$C_{re(i)} = \frac{N}{n} \tag{11}$$

where $C_{re(i)} = 1$ if there is only one report in one row.

$C_{Ne}$ describes the cluster's energy correlations and is defined as follows:

$$C_{Ne} = \prod C_{re(i)} \tag{12}$$

where $C_{re(i)}$ is the energy correlations in each row.

The correlations coefficient $C$ measures the spatial and temporal correlations in a cluster and is defined as follows:

$$C = C_{Nt} \times C_{Ne} \tag{13}$$

If $C$ is greater than a threshold, the collected data are considered having correlations. Then the temporal cluster head reports the result to its static cluster head, and the cluster head will report the detection to the sink eventually.

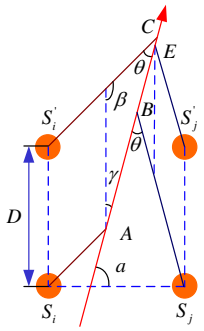


Figure 10: Ship speed estimation

*2) The ship speed estimation:* As described in section II, the angle between the locus of cusps and the sailing line is constantly fixed. Via this characteristic and the multi-node correlated information collected by the temporary cluster head, we can estimate the speed of the intrusion ship.

We assume the network are deployed manually as Fig. 9 shows. We also assume that the ship's sailing line forms an angle of $\alpha$ with the line of two nodes as shown in Fig. 10. We assume that nodes in the network are time-synchronized. At point $A$, the ship waves are detected by sensor $S_i$ at time $t_1$. When the ship arrives at point $C$, its waves were detected by sensor $S_i^{'}$ at time $t_2$. Thus the ship sails from point A to point C during a time period of $t_2 - t_1$. We assume the speed of the ship is $v$. Then, we obtain

$$v = \frac{|AC|}{t_2 - t_1}.$$

Using sine theorem, we calculate $|AC|$ as

$$\frac{|AC|}{sin\beta} = \frac{D}{sin\theta}$$

Using geometry, we obtain

$$\gamma = 90^\circ - \alpha, \theta = 20^\circ, \beta = 70^\circ + \alpha.$$

We have

$$\begin{aligned} v &= \frac{|AC|}{t_2 - t_1} \\ &= \frac{Dsin\beta}{(t_2 - t_1)sin\theta} \\ &= \frac{Dsin(70^\circ + \alpha)}{(t_2 - t_1)sin\theta} \end{aligned} \tag{14}$$

Just the same, from Fig. 10 we observe that the ship waves are detected by sensor $S_j$ at time $t_3$. When the ship arrives at point $E$, the sensor $S_j^{'}$ detects the waves at time $t_4$. Using the same method, we obtain the equation below:

$$\begin{aligned} v &= \frac{|BE|}{t_4 - t_3} \\ &= \frac{Dsin\beta}{(t_4 - t_3)sin\theta} \\ &= \frac{Dsin(\alpha - 70^\circ)}{(t_4 - t_3)sin\theta} \end{aligned} \tag{15}$$

Combining Equation (14) and (15) we have the speed of the ship $v$ as following equation:

$$\begin{cases} v = \frac{Dsin(\alpha - 70^\circ)}{(t_4 - t_3)sin\theta} \\ \alpha = \arctan(\frac{t_2 + t_4 - t_1 - t_3}{t_2 + t_3 - t_1 - t_4} \tan 70^\circ) \end{cases} \tag{16}$$

where $\theta$ is $20^\circ$.

As for the moving direction of the ship, it is easy to obtain with the timestamps of the four nodes.

**Algorithm SID**

**procedure** INITIALIZATION
  *Initialize parameters* $\beta_1, \beta_2, C_{max}$
  *Sample u data*
  *Compute* $m_{\Delta t}, d_{\Delta t}$ *using equation* (4)
  $DetectIntrusion()$
  **return** TRUE
**end procedure**
**procedure** DETECTINTRUSION
  *Sample data* $\alpha_i$
  *Compute* $D_i$ *using equation* (13)
  **if** $a_f$ *passes predefined threshold* **then**
    **if** $NotInTempCluster$ **then**
      $SetUpTempCluster()$
    **else**
      $ReportDetectToTempClusterHead$
    **end if**
  **else**
    **if** *Samples reach predefined number* **then**
      *Compute* $m_T^{'}, d_T^{'}$ *using equation*(5)
    **end if**
  **end if**
  **return** TRUE
**end procedure**
**procedure** SETUPTEMPCLUSTER
  $Inform\ nodes\ within\ six\ steps$
  $NotInTempCluster = False$
  $TempClusterHead = True$
  $TimerTickOn = True$
  **return** TRUE
**end procedure**
**procedure** SPACETIMEDATAPROCESSING
  **if** $TimeTickOn = False$
    and $SpaceTimeCondition = True$
    and $SpaceTimeDataRelated() = True$ **then**
    $DetectionReportToLocalClusterHead()$
  **end if**
  **if** $ShipSpeedCondition = True$ **then**
    *Compute speed using equation*(16)
  **end if**
  **return** TRUE
**end procedure**

### D. The algorithm

In this section, we present the algorithm SID in detail. An intrusion detection algorithm should include algorithms of node and sink. For simplicity, we only present the node's algorithm here. The algorithm includes initialization of node, intrusion detection, temporary cluster setup, correlation of spatial and temporal data processing.

The Initialization procedure deals with initialization of nodes. It first initializes parameters such as $\beta_1, \beta_2, C_{max}$. After that, node samples a number of $u$ data, then computes $m_{\Delta t}, d_{\Delta t}$ using equation (4). At last the node starts up intrusion detection procedure.

The procedure of intrusion detection includes two tasks. First, the node samples data $a_i$ and then computes $D_i$ using $equation$ (13). If $a_f$ passes the predefined threshold within a certain period of time, the node either reports it to its temporary cluster head, or starts to set up a temporary cluster itself. Second, if $D_i$ is normal, $a_i$ will be stored. When the number of sampled data reaches a predefined number, the node computes $m_T^{'}, d_T^{'}$ using $equation$ (5).

The procedure of SetUpTempCluster is to set up the cluster within the the temporary cluster's six hops of neighbors. $TimeTickOn$ is a timer and when it reaches a predefined time, the procedure of SpaceTimeDataProcessing can start.

The procedure of SpaceTimeDataProcessing deals with correlation of spatial and temporal data. If the data correlation is satisfied within a certain period of time, the temporary head reports the detection to its local cluster head. Meanwhile if the ship computing condition is satisfied, it computes the speed of the ship using $equation$ (16).

## V. Performance Evaluation

In this section, we evaluate the detection system. We provide quantitative analysis based on the real data which we collected at our initial experiments as discussed in section III-A. We evaluate node-level detection, cluster-level detection respectively.

### A. Node-level evaluation

In node-level evaluation, we evaluate the successful detection ratio of a node. The node's deployment distance D is 25m. As the ship-waves actually are a train of waves, it disturbs nodes for a short period of time continually. As we observed in the experiment, the time lasts 2-3 seconds. Thus, we take the value as 2 seconds.

The relationship between the anomaly frequency and the successful detection ratio of a node is presented in Fig. 11. From the figure, we observe that as the anomaly frequency $a_f$ increases, the successful detection ratio also increases. The reason is that the anomaly frequency reflects the disturbance level of the train of the ship waves.

If we fix the anomaly frequency, as M increases, the successful detection ratio will increase. This is because if the threshold is higher, the noise of the ocean waves has less impact on the detection, so the successful detection ratio of each node is improved. However, fewer nodes will detect the ship waves especially when the nodes are far from the ship travel line. Due to the noise of the ocean, each node can not have a very high detection accuracy. Thus, our design does not depend too much on individual node's detection accuracy. Observed from the figure, when M=2 and $a_f$=60%, the successful detection ratio is above 70%. Though this detection ratio is not very high, with more nodes in the cluster detecting the ship waves cooperatively, such node-level detection ratio is sufficient to guarantee a successful cluster level detection. We will discuss it in next section.

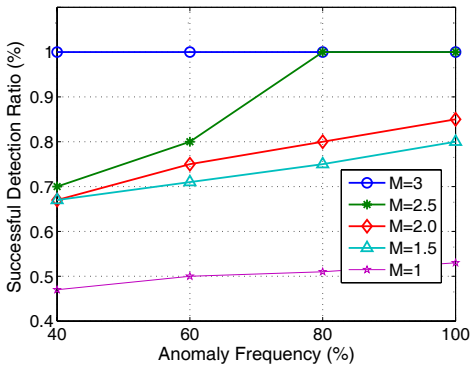


Figure 11: The relationship between anomaly frequency and success detection ratio

### B. Cluster-level evaluation

At the node-level detection, to get a high probability of detection, the false alarm will increase which lead to a low success detection ratio. However, with more nodes detecting the ship cooperatively, the false alarm decreases, thus improves the reliability of the detection, especially by exploiting the spatial and temporal correlations in the collected data. We evaluate the impact of correlations coefficient $C$ and estimate the speed of the ship in this section.

*1) The impact of correlations coefficient C:* To valuate the impact of $C$, we first evaluate the sampled data without ship intrusion. We low the threshold in order to have higher false alarm reports. We process 5 nodes' data in each row and compute correlation coefficient $C$ from 4 to 6 rows respectively with different M.

The results are presented in Table I. The results show that though there are false alarm reports when there is no ship intrusion, the data have a very low correlations coefficient $C$. This is because these false alarms are randomly distributed data, and they have little correlation as for their occurred time and energy level.

Next, we evaluate the data with ship intrusions of different ship speeds. We compute the correlation coefficient for each speed, and then average the coefficient. The results are presented in Table II. Compared with Table I, the data have

Table I: The correlation coefficient without ship intrusion

| $M$ | row=4 | row=5 | row=6 |
|---|---|---|---|
| 1 | 0.019 | 0.013 | 0.006 |
| 2 | 0.009 | 0.005 | 0.001 |
| 3 | 0.002 | 0 | 0 |

Table II: The correlation coefficient with ship intrusion

| $M$ | row=4 | row=5 | row=6 |
|---|---|---|---|
| 1 | 0.62 | 0.53 | 0.47 |
| 2 | 0.75 | 0.69 | 0.60 |
| 3 | 0.81 | 0.72 | 0.68 |

an higher value of spatial and temporal correlations $C$ with ship intrusions. The results also reveal that as M increases, the correlation coefficient also increases. The reason is that as M increases, more false positive reports will be filtered out.

Summarized from Table I and Table II, in the cluster-level detection, if the cluster consists of at least 4 rows of nodes, the cluster-head can report the detection to the sink when the correlation coefficient $C$ exceeds 0.4.

*2) Ship speed estimation:* The evaluation data are collected by 4 deployed nodes and the deployment distance D is 25m, as Fig. 10 shows. The ship uses two speed levels that are about 10 knots and 16 knots respectively, and it travels through the network with different angle and speeds to generate data for ship speed estimation.

As to each test, we only record the reports which have the highest detected energy within the test period of time. Then we use $equation$ (16) to compute the speed of the ship.

Fig. 12 shows the actual speed of the ship and the estimated speed of the ship. For the 10 knots test, the computed speed of the ship is between 8 to 12 knots. As to 16 knots test, the figure is from 15 to 18 knots. The estimated velocity of the ship is close to the actual speed of the ship, but there are errors. There are two reasons for the estimated errors: First, the ship's traveling line is not really a straight line due to the sea waves. Second, for the same reason, the nodes deployed in the sea are not static and have about 2 meters free drifting radius with the waves [21]. Though there are errors in the estimation, the errors are within $20\%$ of the actual speed of the ship.

## VI. Related work

In this section, we introduce some researches related to our paper. The researches on detection, classification and target tracking with deployment of WSNs has received a considerable amount of attention recently, and some researchers have deployed a number of successful real-world systems [1]–[3]. Arora et. al. introduce the concept of influence field,

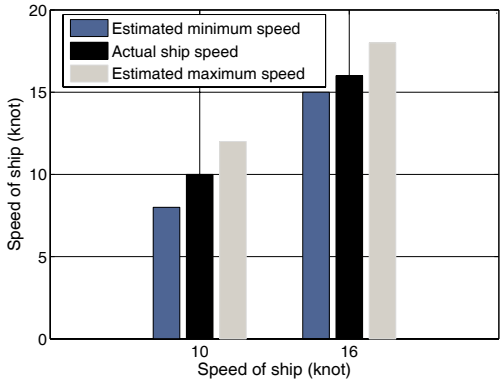


Figure 12: Ship speed estimation

which can be estimated from a network of binary sensors [2]. They use the influence field as the basis of their novel classifier. Gu et. al. design a light-weighted hierarchical classification architecture that naturally distributes sensing and computation tasks at different levels of the system with VigiNet [1]. Marco et. al. studied a vehicle classification based on the data set collected at the third SensIT program [3]. Zhang et. al. deployed a ZebraNet for wild animal tracking [22]. He et. al. developed a surveillance network which can detect moving targets [23]. Dutta et. al. deployed the Extreme Scaling WSNs which employ a heterogeneous network topology to detect exceptional events [24]. Zhu et. al. present an innovative scheme to tackle online real-time vehicle tracking problem [25].

The above mentioned researches are all designed for terrestrial wireless sensor networks. There are a few researches dealing with intrusion detection on the water. In [26], the authors describe a coastal sensor network to detect, classify, and track submerged threat objects. The unattended in-water sensors first perform the initial and coarse target detection, then the shore based optical sensors develop refined track on the targets. Barry et. al. developed an experiment on the Hudson River Estuary to detect ships [27]. Their system combines a specialized prototype video system and a passive underwater acoustic sensor network to track and classify ships on the river.

The ship-generated waves have been an old research topic [7], [8]. But the prior researches mainly focused on the harm of the ship-generated waves, such as reducing wave resistance for ship hull design, or preventing damage of coastal or marine floating structures etc [8]. In this paper, we leverage the characteristics of the ship waves to detect passing ships.

## VII. Conclusions and Future Work

In this paper, we present the intrusion detection system on the sea by using three-axis accelerometer sensors. By signal processing techniques, the sensors can distinguish

ship-generated waves and ocean waves. Cooperative signal processing also increases the reliability of the system. We design an intrusion detection system which exploits the spatial and temporal correlations of the intrusion to increase detection reliability. We also conduct evaluations with real data collected by our initial experiments, and provide quantitative analysis of the system, such as the successful detection ratio and the estimation of the speed of the intruding ships.

Though the adaptive threshold design deals with different kinds of weather, we need further experiments with bad weathers. We also need to explore the data collected by individual nodes further and to combine accelerometer sensor with acoustic sensor underwater, which we are building and testing now, to detect ship intrusions cooperatively. The current design can not support online intrusion detection, we leave it as our future work.

## ACKNOWLEDGMENT

This research was supported in part by China NSFC Grants 60873248, 60933011, 60970129 and 60933012, Hong Kong RGC Grants 617908 and 617710.

## REFERENCES

[1] L. Gu, D. Jia, P. Vicaire, T. Yan, L. Luo, A. Tirumala, Q. Cao, T. He, J. Stankovic, T. Abdelzaher *et al.*, "Lightweight detection and classification for wireless sensor networks in realistic environments," in *Proceedings of the 3rd international conference on Embedded networked sensor systems (SenSys'05)*. ACM, 2005, pp. 205–217.

[2] A. Arora, P. Dutta, S. Bapat, V. Kulathumani, H. Zhang, V. Naik, V. Mittal, H. Cao, M. Demirbas, M. Gouda *et al.*, "A line in the sand: A wireless sensor network for target detection, classification, and tracking," *Computer Networks*, vol. 46, no. 5, pp. 605–634, 2004.

[3] M. Duarte and Y. Hen Hu, "Vehicle classification in distributed sensor networks," *Journal of Parallel and Distributed Computing*, vol. 64, no. 7, pp. 826–838, 2004.

[4] S. Kumar, T. Lai, and A. Arora, "Barrier coverage with wireless sensors," in *Proceedings of the 11th annual international conference on Mobile computing and networking (MobiCom'05)*. ACM, 2005, pp. 284–298.

[5] Z. Yang, M. Li and Y. Liu, "Sea depth measurement with restricted floating sensors," in *Proceedings of 28th IEEE International Real-Time Systems Symposium (RTSS'07)*. IEEE, 2007, pp. 469–478.

[6] B. Malhotra, I. Nikolaidis, and J. Harms, "Distributed classification of acoustic targets in wireless audio-sensor networks," *Computer Networks*, vol. 52, no. 13, pp. 2582–2593, 2008.

[7] F. Ursell, "On Kelvin's ship-wave pattern," *Journal of Fluid Mechanics Digital Archive*, vol. 8, no. 03, pp. 418–431, 2006.

[8] A. Velegrakis, M. Vousdoukasa, A. Vagenasa, T. Karambasa, K. Dimoua, and T. Zarkadasa, "Field observations of waves generated by passing ships: A note," *Coastal Engineering*, vol. 54, pp. 369–375, 2007.

[9] T. Havelock, "The propagation of groups of waves in dispersive media, with application to waves on water produced by a travelling disturbance." The Royal Society, 1908, pp. 398–430.

[10] R. Sorensen, "Water waves produced by ships," *Journal of the Waterways, Harbors and Coastal Engineering Division*, vol. 99, no. 2, pp. 245–256, 1973.

[11] A. T. Chwang and Y. Chen, "Field Measurement of Ship Waves in Victoria Harbor," *Journal of Engineering Mechanics*, vol. 129, pp. 1138–1148, 2003.

[12] "IMote2: http://ubi.cs.washington.edu/wiki/index.php/IMote2"

[13] B. Hubbard and F. Meyer, *The world according to wavelets: the story of a mathematical technique in the making*. AK Peters Wellesley, 1996.

[14] S. Massel, "Wavelet analysis for processing of ocean surface wave records," *Ocean Engineering*, vol. 28, no. 8, pp. 957–987, 2001.

[15] Y. Meyer, S. Jaffard, and O. Rioul, "L'analyse par ondelettes," *Pour la science*, vol. 119, pp. 28–37, 1987.

[16] Y. Liu, K. Liu and M. Li, "Passive diagnosis for wireless sensor networks," *IEEE/ACM Transactions on Networking*, vol. 18, no. 4, pp. 1132–1144, 2010.

[17] H. Luo, Z. Guo, K. Wu, F. Hong, Y. Feng, "Energy Balanced Strategies for Maximizing the Lifetime of Sparsely Deployed Underwater Acoustic Sensor Networks," *Sensors*, vol. 9, no. 9, pp. 6626–6651, 2009.

[18] H. Luo, Y. Zhao, Z. Guo, S. Liu, P. Chen and Lionel M. Ni, "Udb: using directional beacons for localization in underwater sensor networks," in *Proceedings of the 14th IEEE International Conference on Parallel and Distributed Systems(ICPADS'08)*. IEEE, 2008, pp. 551–558.

[19] K. Wu, H. Tan, Y. Liu, Q. Zhang, and Lionel M. Ni, "Side Channel: Bits over Interference," in *Proceedings of the 16th Annual International Conference on Mobile Computing and Networking (MobiCom'10)*. IEEE, 2010.

[20] K. Wu, H. Tan, H. Ngan and Lionel M. Ni, "Chip Error Patterns Analysis in IEEE 802.15.4," in *Proceeding of the 29th Conference on Computer Communications (Infocom'10)*. IEEE, 2010.

[21] H. Luo, Z. Guo, W. Dong, F. Hong and Y. Zhao, "Ldb: Localization with directional beacons for sparse 3d underwater acoustic sensor networks," *Journal of Networks*, vol. 5, no. 1, pp. 28–38, 2010.

[22] P. Zhang, C. Sadler, S. Lyon, and M. Martonosi, "Hardware design experiences in ZebraNet," in *Proceedings of the 2nd international conference on Embedded networked sensor systems (SenSys'04)*. ACM, 2004, pp. 227–238.

[23] T. He, S. Krishnamurthy, J. Stankovic, T. Abdelzaher, L. Luo, R. Stoleru, T. Yan, L. Gu, J. Hui, and B. Krogh, "Energy-efficient surveillance system using wireless sensor networks," in *Proceedings of the 2nd international conference on Mobile systems, applications, and services (MobiSys'04)*. ACM, 2004, pp. 270–283.

[24] P. Dutta, M. Grimmer, A. Arora, S. Bibyk, and D. Culler, "Design of a wireless sensor network platform for detecting rare, random, and ephemeral events," in *Proceedings of the 4th international symposium on Information processing in sensor networks (IPSN'05)*. IEEE, 2005.

[25] H. Zhu and Lionel M.Ni, "HERO: Online Real-Time Vehicle Tracking in Shanghai," in *Proceeding of the 27th Conference on Computer Communications (Infocom'08)*. IEEE, 2008, pp. 942–950.

[26] E. Carapezza, J. Butman, I. Babb, and A. Bucklin, "Sustainable coastal sensor networks: technologies and challenges," in *Proceedings of SPIE*, vol. 6963, 2008.

[27] B. Bunin, A. Sutin, G. Kamberov *et al.*, "Fusion of acoustic measurements with video surveillance for estuarine threat detection," in *Proceedings of SPIE*, vol. 6945, 2008.